

Lewis Acid Mediated Hydrosilylation on Porous Silicon Surfaces

Jillian M. Buriak,^{*,†} Michael P. Stewart,[†] Todd W. Geders,[†] Matthew J. Allen,[†] Hee Cheul Choi,[†] Jay Smith,[†] Daniel Raftery,^{*,†} and Leigh T. Canham^{*,‡}

Contribution from the Department of Chemistry, 1393 Brown Laboratories, Purdue University, West Lafayette, Indiana 47907-1393, and the Defence Evaluation Research Agency (DERA) Malvern, St. Andrews Road, Malvern, Worcestershire, WR14 3PS, United Kingdom

Received June 25, 1999

Abstract: Lewis acid mediated hydrosilylation of alkynes and alkenes on non-oxidized hydride-terminated porous silicon derivatizes the surface with alkenyl and alkyl functionalities, respectively. A very broad range of chemical groups may be incorporated, allowing for tailoring of the interfacial characteristics of the material. The reaction is shown to protect and stabilize porous silicon surfaces from atmospheric or direct chemical attack without compromising its valuable material properties such as high porosity, surface area and visible room-temperature photoluminescence. The reaction is shown to act on alkenes and alkynes of all possible regiochemistries (terminal and internal alkynes; mono-, *cis*- and *trans*-, di-, tri-, and tetrasubstituted alkenes). FTIR as well as liquid- and solid-state NMR spectroscopies show anti-Markovnikov addition and *cis* stereochemistry in the case of hydrosilylated terminal alkynes. Material hydrosilylated with long-chain hydrophobic alkynes and alkenes shows a substantially slower surface oxidation and hydrolysis rate in air as monitored by long-term FTIR monitoring and chemography. BJH and BET measurements reveal that the surface area and average pore size of the material are reduced only slightly after hydrosilylation, indicating that the porous silicon skeleton remains intact. Elemental analysis and SIMS depth profiling show a consistent level of carbon incorporation throughout the porous silicon which demonstrates that the reaction occurs uniformly throughout the depth of the film. The effects of functionalization on photoluminescence were investigated and are shown to depend on the organic substituents.

Introduction

Porous silicon is a high surface area morphology of hydride terminated silicon whose efficient room-temperature luminescence has attracted much interest for a wide range of applications.¹ Initial excitement in the early 1990s focused upon the potential to use light-emitting silicon in optoelectronic devices that could be easily integrated with existing silicon-based technology.² While still heavily debated in the literature, light emission most likely results from quantum confinement effects within silicon nanocrystallites and nanowires imbedded within the porous matrix.³ Since the discovery of light emission, porous silicon has been shown to serve as the platform for a broad range of applications, such as sensing and bioanalysis, utilizing a number of different signal transduction schemes. For instance, Sailor and Harper demonstrated the sensitivity of the photoluminescence (PL) efficiency with respect to NO concentration in Ar, rendering porous silicon a useful chemosensor for this compound and other gases.⁴ By functionalizing oxidized porous silicon surfaces with biological molecules such as biotin and single-stranded DNA, porous silicon can act as an effective

optical interferometric biosensor for quantifying streptavidin and a complementary strand of DNA, respectively, as shown by Sailor and Ghadiri.⁵ Recently, Buriak and Siuzdak discovered that porous silicon can replace the organic matrix in MALDI (matrix-assisted laser desorption/ionization) mass spectrometry which allows for high sensitivity and remarkable salt tolerance, with the added advantage of integration of the porous silicon into silicon wafer-based microfluidic devices for on-chip analysis.⁶ Widespread application of porous silicon is contingent, however, upon the stabilization of the material which deteriorates in ambient conditions due to oxidation and adsorption of impurities from the air.⁷ Corrosion of porous silicon in aqueous solution, and especially in simulated biological conditions, occurs even more rapidly, and thus a general method to stabilize the surface is crucial for some applications such as biosensing and biofiltration.⁸ Ideally, the methodology should not only render the surface robust but should also allow for incorporation of a broad range of chemical functionalities upon demand to tailor the surface for specific applications. The ability to controllably and permanently attach organic molecules to nanocrystalline silicon surfaces is also interesting within the burgeoning field of nanotechnology and for creation of molecular-scale architectures on semiconductor substrates.

Because monolayers on single-crystal non-oxidized silicon surfaces bound through silicon-carbon bonds have been shown

[†] Purdue University.

[‡] DERA.

(1) (a) *Properties of Porous Silicon*; Canham, L. T., Ed.; INSPEC: London, 1997. (b) *Structural and Optical Properties of Porous Silicon Nanostructures*; Amato, G.; Delerue, C.; von Bardeleben, H.-J., Eds.; Gordon and Breach: Amsterdam, 1997.

(2) (a) Canham, L. T. *Appl. Phys. Lett.* **1990**, *57*, 1046. (b) Lehmann, V.; Gosele, U. *Appl. Phys. Lett.* **1991**, *58*, 856. (c) Halimaoui, A.; Oules, C.; Bomchil, G.; Bsiesy, A.; Gaspard, F.; Hérino, R.; Ligeon, M.; Muller, F. *Appl. Phys. Lett.* **1991**, *59*, 304.

(3) Sailor, M. J.; Lee, E. J. *Adv. Mater.* **1997**, *7*, 783.

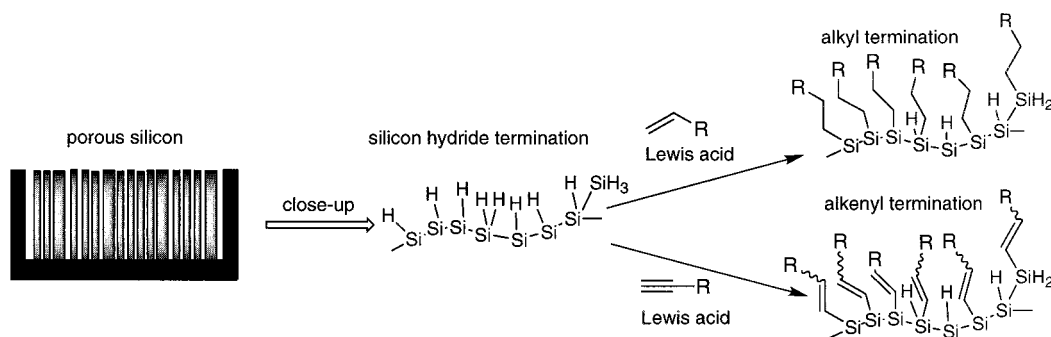
(4) Harper, J.; Sailor, M. J. *Anal. Chem.* **1996**, *68*, 3713.

(5) Janshoff, A.; Dancil, K. P. S.; Steinem, C.; Greiner, D. P.; Lin, V. S. Y.; Gurtner, C.; Motesharei, K.; Sailor, M. J.; Ghadiri, M. R. *J. Am. Chem. Soc.* **1998**, *120*, 12108.

(6) Wei, J.; Buriak, J. M.; Siuzdak, G. *Nature* **1999**, *399*, 243.

(7) Canham, L. T. In *Properties of Porous Silicon*; Canham, L. T., Ed.; INSPEC: London, 1997; pp 44–50.

(8) Canham, L. T. *Adv. Mater.* **1995**, *7*, 1033.

Scheme 1. Cartoon Cross Section of Porous Silicon^a

^a Native surface is hydride-terminated, and in the presence of the Lewis acid EtAlCl_2 , insertion of an alkyne or an alkene takes place, resulting in alkenyl- or alkyl-terminated surfaces, respectively.

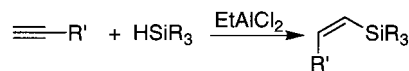
to result in extremely stable flat surfaces,⁹ a similar approach has been pursued on porous silicon.¹⁰ The nanoscale architecture of porous silicon is inherently fragile, and thus rapid and efficient syntheses under room-temperature conditions are preferable. Previous approaches taken toward Si–C bond formation on porous silicon include reactions with methyl Grignard under electrochemical conditions,¹¹ alkyl and aryl-lithium and Grignard reagents in the absence of electronic bias,¹² and thermal hydrosilylation of alkynes and alkenes.¹³ We have found that hydrosilylation of unsaturated carbon–carbon bonds on the native hydride-terminated porous silicon can be induced by the Lewis acid EtAlCl_2 ¹⁴ or white light illumination (on photoluminescent samples)¹⁵ at room temperature in a matter of minutes or hours, depending upon the organic fragment, as outlined in Scheme 1. Insertion of alkenes or alkynes into surface Si–H groups yields alkyl or alkenyl termination, respectively. Both chemistries are remarkably tolerant of a wide range of chemical functionalities and are complementary, which allows for flexibility in choosing specific surface properties. The hydrophobic surfaces capped with a monolayer of long alkyl chains were reported to be dramatically stabilized under chemically demanding, basic conditions as compared to unfunctionalized porous silicon. In this paper, we thoroughly explore the scope of the Lewis acid hydrosilylation reaction and utilize FTIR and solid-state ¹³C CP/MAS NMR to characterize the surface bound organic moieties. Surface hydrosilylations mediated by EtAlCl_2 act upon terminal, *cis*- and *trans*-disubstituted, trisubstituted, and tetrasubstituted alkenes and terminal and internal alkynes. The stereochemistry of the hydrosilylation of terminal alkynes and alkenes has been investigated with IR and NMR techniques, and through the latter, strong evidence for the covalent attachment of organic functionalities to a silicon surface via silicon–carbon bonds is revealed. Correlations of the proposed surface species with

analogous soluble, solution-phase compounds have been made to further substantiate their structures.

The consequences of monolayer formation on the high surface area network and average pore size of porous silicon have been measured by Brunauer–Emmett–Teller (BET) and Barrett–Joyner–Halenda (BJH) gas adsorption methods which show that functionalization occurs without changing its porous structure.¹⁶ Secondary ion mass spectrometry (SIMS) depth profiling,¹⁷ indicates that hydrosilylation takes place uniformly throughout the material. In our earlier contribution, we had only demonstrated increased resistance with respect to alkali. In this work, enhanced stability with respect to oxidation in ambient, laboratory conditions in air through both FTIR and chemographic means is revealed. The effects of the functionalization on the intrinsic photoluminescence are also detailed here.

Results and Discussion

The Hydrosilylation Reaction. Hydrosilylation of alkynes mediated by the Lewis acid EtAlCl_2 was initially communicated, utilizing soluble, molecular trisubstituted silanes such as triethylsilane, $(\text{CH}_3\text{CH}_2)_3\text{SiH}$.¹⁸ The reaction in solution adds exclusively *trans* in an anti-Markovnikov fashion, and thus with a terminal alkyne, yields the *cis* product as determined by ¹H NMR.



The solution-phase reaction conditions are extremely gentle, which initially suggested that this reaction would be ideal for the fragile porous silicon surfaces. By adapting these conditions to freshly etched hydride-terminated porous silicon, hydrosilylation of alkynes rapidly takes place (<1 h) at room temperature, as evidenced by the decrease in intensity of the $\nu(\text{Si}-\text{H}_x)$ stretch centered around 2100 cm^{-1} and appearance of new vibrations in the transmission FTIR spectrum which correspond to the alkenyl substitution, shown in Figure 1a–c. Lewis acid mediated hydrosilylation of alkenes also occurs but requires longer reaction times, on the order of at least 12 h at room tempera-

(9) Organic monolayers on flat silicon, demonstrating increased stability: (a) Sieval, A. B.; Demirel, A. L.; Nissink, J. W. M.; Linford, M. R.; van der Maas, J. H.; de Jeu, W. H.; Zuilhof, H.; Sudholter, E. J. R. *Langmuir* **1998**, *14*, 1759–1768. (b) Linford, M. R.; Fenter, P.; Eisenberger, P. M.; Chidsey, C. E. D. *J. Am. Chem. Soc.* **1995**, *117*, 3145–3155. (c) Bansal, A.; Li, X.; Lauermann, I.; Lewis, N. S.; Yi, S. I.; Weinberg, W. H. *J. Am. Chem. Soc.* **1996**, *118*, 7225.

(10) For a general review of organometallic chemistry on silicon surfaces, see: Buriak, J. M. *J. Chem. Soc., Chem. Commun.* **1999**, 1051.

(11) Ozanam, F.; Vieillard, C.; Warntjes, M.; Dubois, T.; Pauly, M.; Chazalviel, J.-N. *Can. J. Chem. Eng.* **1998**, *76*, 1020.

(12) (a) Song, J. H.; Sailor, M. J. *J. Am. Chem. Soc.* **1998**, *120*, 2376. (b) Song, J. H.; Sailor, M. J. *Inorg. Chem.* **1999**, *38*, 1498. (c) Kim, N. Y.; Laibinis, P. E. *J. Am. Chem. Soc.* **1998**, *120*, 4516.

(13) Bateman, J. E.; Eagling, R. D.; Worrall, D. R.; Horrocks, B. R.; Houlton, A. *Angew. Chem., Int. Ed.* **1998**, *37*, 2683.

(14) Preliminary communication: Buriak, J. M.; Allen, M. J. *J. Am. Chem. Soc.* **1998**, *120*, 1339.

(15) Stewart, M. P.; Buriak, J. M. *Angew. Chem., Int. Ed.* **1998**, *37*, 3257.

(16) (a) Hérino, R. In *Properties of Porous Silicon*; Canham, L. T., Ed.; INSPEC: London, 1997; pp 89–96. (b) Barrett, E. P.; Joyner, L. G.; Halenda, P. P. *J. Am. Chem. Soc.* **1951**, *73*, 373.

(17) Canham, L. T.; Houlton, M. R.; Leong, W. Y.; Pickering, C.; Keen, J. M. *J. Appl. Phys.* **1991**, *70*, 422.

(18) (a) Asao, N.; Sudo, T.; Yamamoto, Y. *J. Org. Chem.* **1996**, *61*, 7654. (b) Sudo, T.; Asao, N.; Gevorgyan, V.; Yamamoto, Y. *J. Org. Chem.* **1999**, *64*, 2494.

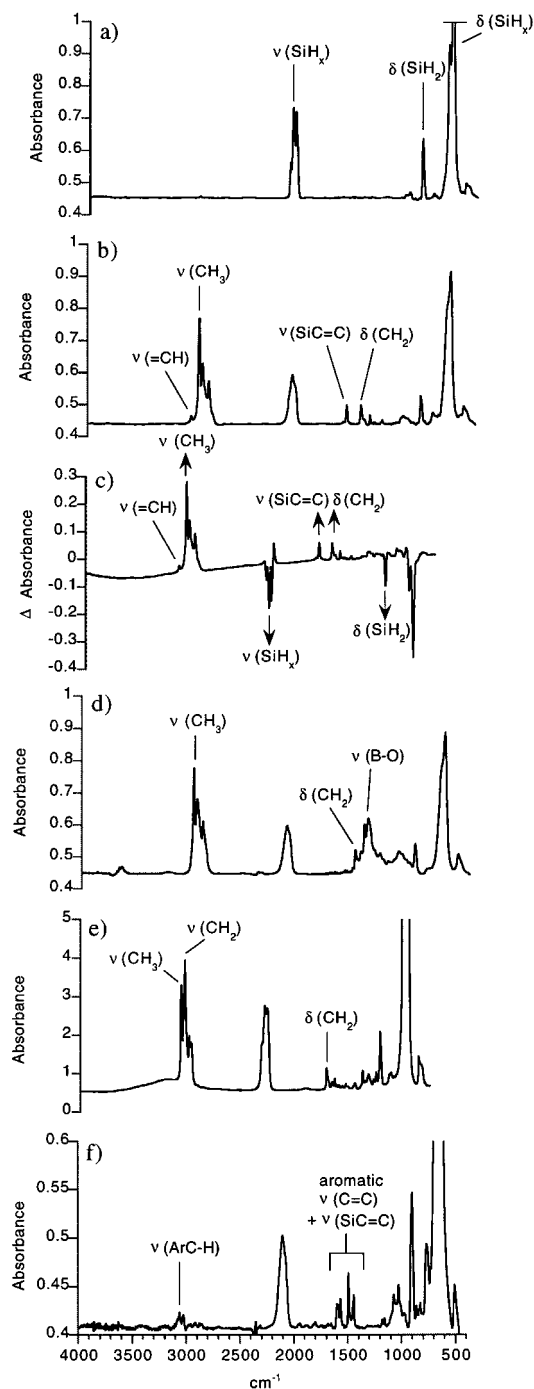


Figure 1. Transmission FTIR spectra of porous silicon upon Lewis acid mediated hydrosilylation with EtAlCl₂ and an alkyne or alkene. (a) Sample of freshly etched, Si-H_x terminated porous silicon, prepared through etching procedure D(a) (Experimental Section) with no further reaction. (b) The sample from (a) upon reaction with 1-pentene, resulting in pentenyl derivatization. (c) Difference spectrum of spectrum (a) subtracted from sample (b), indicating disappearance of ν(Si-H_x) intensity and appearance of features corresponding to the pentenyl termination. (d) The sample from (b) upon hydroboration with THF·BH₃, resulting in complete disappearance of the ν(SiC=C) at 1595 cm⁻¹. (e) A porous silicon sample prepared through etch D(a) upon reaction with 1-pentene, resulting in pentyl termination. (f) Porous silicon prepared through etch A and reacted with phenylacetylene, resulting in styrenyl termination. The same porous silicon sample was used for the spectra (a)–(d) and etched and reacted in a homemade Teflon cell which doubled as an IR sample holder. This enabled the same spot to be analyzed each time, allowing for meaningful comparisons of changes in absolute intensity.

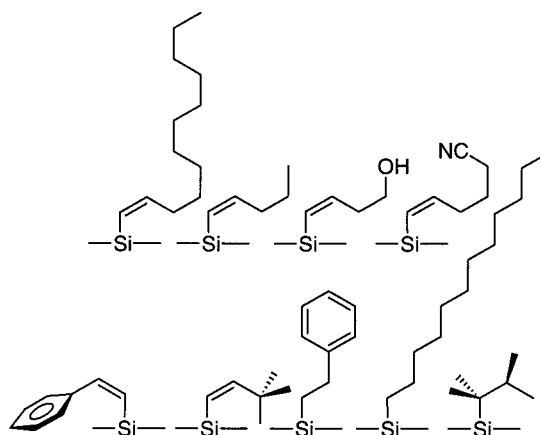


Figure 2. Examples of the surface terminations possible through Lewis acid mediated hydrosilylation on porous silicon.

ture.¹⁹ These hydrosilylation conditions are tolerant of a wide range of functional groups within the alkyne or alkene, as demonstrated by the range of surfaces prepared, shown in Figure 2. Lewis basic functionalities require an excess of Lewis acid since one equivalent complexes the Lewis base. Late transition metal complexes, commonly used for solution-phase hydrosilylation reactions, are inferior to the Lewis acid EtAlCl₂ because they induce total quenching of photoluminescence and substantial oxidation, presumably due to deposition of reduced metal on the surface.²⁰ The hydrosilylation reaction is successful on all porous silicon samples tried thus far, regardless of initial doping. A wide range of morphologies have been tried and tested, including micro-, meso-, and macroporous samples.²¹ In all cases, little oxidation is noted in these reactions which is extremely advantageous for the production of stabilized surfaces. The ability of the Lewis acid to scavenge trace water which could otherwise add across weak Si-Si bonds is almost certainly an important factor in reducing competing, concomitant oxidation.²²

Other Lewis acids were not found to be as effective as these aluminum based compounds. For instance, tris(pentafluorophenyl)borane is a strong Lewis acid catalyst that has been shown to be effective for hydrosilylation of ketone substrates in solution and was therefore tested for hydrosilylation reactions on porous silicon.²³ Utilization of tris(pentafluorophenyl)borane (0.4 M solution in hexane) as the Lewis acid mediator for phenylacetylene hydrosilylation was only mildly effective—minor incorporation of styrenyl moieties on the surface was noted by FTIR. BF₃·etherate was also shown to be ineffective for mediating surface hydrosilylation of alkynes.

FTIR Analysis. Hydrosilylation of alkynes on porous silicon yields surface bound vinyl groups as revealed by the observation of a strong vibration in the transmission FTIR spectrum at ~1600 cm⁻¹, indicative of a monosilyl-substituted carbon-carbon double bond ν(SiC=C).²⁰ As shown by Figure 1b and c, the surface-bound vinyl group formed upon hydrosilylation of 1-pentene appears at 1595 cm⁻¹ and a corresponding vinylic hydrogen ν(C-H) stretch can be observed at 3040 cm⁻¹. Hydrosilylation of other terminal alkyl alkynes yields a similar

(19) (a) Oertle, K.; Wetter, H. *Tetrahedron Lett.* **1985**, 26, 5511. (b) Yamamoto, K.; Takemae, M. *Synlett* **1990**, 259.

(20) Buriak, J. M.; Holland, J. M.; Allen, M. J. Allen, Stewart, M. P. *J. Solid State Chem.* **1999**, 147, 251.

(21) Microporous samples prepared through etching procedures E, mesoporous through A, B, C, and D, and macroporous through ref 5.

(22) Canham, L. T.; Saunders, S. J.; Heeley, P. B.; Keir, A. M.; Cox, T. I. *Adv. Mater.* **1994**, 6, 865.

(23) Parks, D. J.; Piers, W. E. *J. Am. Chem. Soc.* **1996**, 118, 9440.

feature in the FTIR spectra. In the case of aryl alkynes such as phenylacetylene (Figure 1f), the vinyl group overlaps with various ν (C=C) aromatic ring modes and thus cannot be distinguished unambiguously.

To affirm the identity of the surface bound vinyl ν (SiC=C), the related molecular compound, 1-[tris(trimethylsilyl)silyl]-(*Z*)-pentene, the exclusive *cis*-olefinic compound formed from EtAlCl₂-mediated hydrosilylation of 1-pentyne with tris(trimethyl)silylsilane, was synthesized. The carbon-carbon double bond ν (SiC=C) stretch appears at 1594 cm⁻¹ (shown in Supporting Information) which is almost identical to the 1595 cm⁻¹ observed on the porous silicon surface. The absence of the characteristic strong *trans*-olefinic out-of-plane mode, γ_w -(-CH=CH-)_{trans}, in the FTIR at ~970 cm⁻¹ in both the molecular model compound and in the porous silicon spectra is consistent with the *cis* form of the alkenyl group.²⁴ At much higher reaction temperatures (110–200 °C), hydrosilylation can be induced thermally,^{13,20} and formation of the more thermodynamically favored *trans* form is observed. When a dodecyl-terminated surface is prepared with a 2 h reflux in neat dodecylene, hydrosilylation occurs as evidenced by the appearance of the ν (SiC=C), clearly visible at 1601 cm⁻¹, as well as a vibration at 979 cm⁻¹ which is absent in EtAlCl₂ mediated hydrosilylation and is presumably the γ_w -(-CH=CH-)_{trans} (see Supporting Information). In the spectra of EtAlCl₂ mediated alkyne hydrosilylation, a similar out-of-plane mode consistently strong in 1,1'-disubstituted alkenes which appears at 890 cm⁻¹ is also not present and therefore supports anti-Markovnikov addition, as is observed in solution.¹⁸ As would be expected, the surface-bound vinyl group of the pentenyl terminated surface reacts as a double bond, undergoing hydroboration with excess BH₃·THF at room temperature (Figures 1d and 3d). Alkenes are hydrosilylated to yield surface alkyl groups; the reduction in intensity of ν (Si-H_x) and absence of the olefinic ν (SiC=C) stretch substantiates this claim.

The high surface area network of porous silicon is terminated with Si-H_x (x = 1,2,3) bonds. Because the Si-H_x stretching region around 2100 cm⁻¹ becomes substantially broadened and featureless after hydrosilylation, the individual stretches corresponding to ≡SiH, =SiH₂, and -SiH₃ can no longer be distinguished, and as a result, it has not been determined if the reaction exhibits any selectivity with respect to the Si-H_x functionalities. It is important to note, however, that the dissociation energy of the Si-H bonds is known through studies on solution phase silanes to differ in the order of ≡SiH < =SiH₂ < -SiH₃ due to silicon substituent electronic induction.²⁵ This suggests that the ≡SiH groups may have a higher propensity to react selectively based on thermodynamic considerations, although the -SiH₃ groups are the least sterically hindered and so may react more rapidly.

Solid-State ¹³C NMR. While the FTIR analyses strongly support organic surface-bound moieties resulting from hydrosilylation of an alkyne or alkene, solid-state ¹³C NMR provides more detailed information with which to characterize the interfacial species. Previously, EELS and FTIR have been used to attempt to provide direct proof of Si-C bond formation on

(24) For the out-of-plane deformation of *trans*-disubstituted olefins: Bellamy, L. J. *The Infrared Spectra of Complex Molecules*; Chapman and Hall: London, 1975; pp. 50–51. This band has been used extensively to differentiate between *cis*- and *trans*-disubstituted olefins and 1,1'-disubstituted olefins. For the out-of-plane deformation of 1,1'-disubstituted olefins: *ibid.*, p. 57.

(25) (a) Walsh, R. *Acc. Chem. Res.* **1981**, *14*, 246–252. (b) Kanabus-Kaminska, J. M.; Hawari, J. A.; Griller, D.; Chatgililoglu, C. *J. Am. Chem. Soc.* **1987**, *109*, 5267–5268. (c) Chatgililoglu, C. *Acc. Chem. Res.* **1992**, *25*, 188–194.

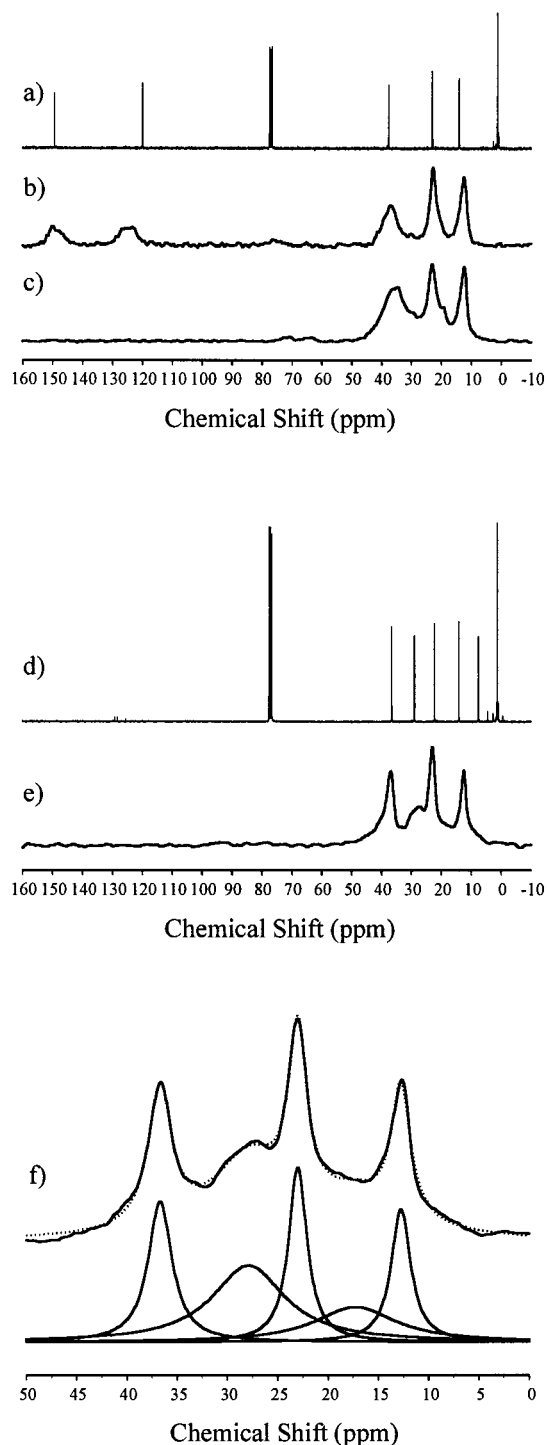
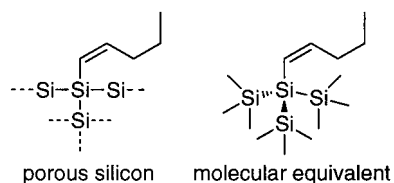


Figure 3. ¹³C NMR spectra. (a) Solution-phase spectrum in CDCl₃ of the coupling product of hydrosilylation of 1-pentyne with tris(trimethylsilyl)silane, catalyzed by EtAlCl₂. (b) Solid-state CP/MAS spectrum of a porous silicon sample upon hydrosilylation of 1-pentyne. (c) Solid-state CP/MAS spectrum after hydroboration of the sample from (b) with BH₃·THF. (d) Solution-phase spectrum in CDCl₃ of the AIBN-mediated hydrosilylation of 1-pentene with tris(trimethylsilyl)silane. (e) Solid-state CP/MAS spectrum of a porous silicon sample upon hydrosilylation of 1-pentene. (f) The aliphatic region of the spectrum shown in (e) with a fit (dotted line) to the data. The decomposition of the fit is shown below and displays 5 distinct resonances.

non-oxidized silicon surfaces, but these techniques are fraught with difficulties due to the low energy and weak intensity of the ν (Si-C) and its corresponding bending modes.^{9c,26} With

solid-state ^{13}C CP/MAS NMR, on the other hand, the resonance for the surface silicon-bound carbon should be clearly distinguishable and would also allow for verification of the structure of the surface-bound organic moieties. Solid-state NMR has been utilized previously to study hydride-terminated and oxidized porous silicon samples as well as adsorbed species on porous silicon.²⁷ In the present work, we focused primarily on the ^{13}C NMR of the chemisorbed organic species as it showed better resolution than is typically observed in the Si spectra of porous silicon, due to its heterogeneous character. Because large masses of porous silicon (> 100 mg) are required for sufficient signal-to-noise ratios in the ^{13}C CP/MAS NMR spectra, four 30 mg samples of porous silicon were etched according to etching procedure D(a) (Experimental Section).

As a representative alkyne, hydrosilylation of 1-pentyne, mediated by EtAlCl_2 , was carried out. The observed ^{13}C CP/MAS NMR spectrum for the derivatized porous silicon was compared to the ^{13}C solution phase NMR in CDCl_3 of a related soluble, molecular equivalent formed from hydrosilylation of the same alkyne by tris(trimethylsilyl)silane. The pentenyl fragment should have very similar ^{13}C NMR profiles since they are both covalently bound to a trisilicon-substituted silicon atom.



The molecule formed from 1-pentyne hydrosilylation with tris(trimethylsilyl)silane has the expected ^{13}C NMR peaks of the two olefinic carbons at δ 149.3 and 119.9 ppm, as shown in Figure 3a. The peak at higher field is attached directly to the silicon atom, as indicated by the observation of ^{29}Si coupling (5% abundance), $^1J_{\text{Si-C}} = 23$ Hz. The remaining three carbons of the propyl aliphatic chain can be seen at 37.7, 23.0, and 14.0 ppm. ^1H NMR confirmed exclusive formation of the (*Z*) olefin, formed through *trans* addition of the Si-H moiety in an anti-Markovnikov fashion.¹⁸ The strong peak at 1.2 ppm is due to the nine methyl groups bound to silicon atoms in the tris(trimethylsilyl)silane fragment.

The ^{13}C CP/MAS solid-state NMR spectrum of the 1-pentyne functionalized porous Si is shown in Figure 3b. A good correlation can be drawn between the peaks in the CP/MAS spectrum and the peaks in the liquids spectrum of the tris(trimethylsilyl)silane analogue. Because of the high similarity of the solid-state ^{13}C NMR and the soluble, molecular equivalent, the solution phase and surface reactions appear to be occurring in an identical manner, yielding the same organic fragment bound through a covalent Si-C bond. Broad resonances from the olefinic carbons are evident at 149.9 and 124.8 ppm. The carbon that is believed to be bonded directly to the

porous Si from the liquid state spectrum, 124.8 ppm, has a line width of nearly 500 Hz while the other olefinic carbon resonance has a line width of about 400 Hz. The broadening of these resonances is most likely due to site heterogeneity at the porous Si surface. The aliphatic resonance at 37.1 ppm also has a line width of over 400 Hz, while the remaining aliphatic carbon, 22.8 ppm and the methyl carbon, 12.6 ppm, have narrower line widths of about 200 Hz. The smaller line widths are due to increased motional averaging and are indicative of the carbons at the end of the propyl group.

Because of the large line widths of the olefinic peaks in the solid-state ^{13}C NMR spectrum, unambiguous assignment of *cis* or *trans* stereochemistry is extremely difficult. Previous work by Chatgililoglu indicates that the olefinic carbons of *cis*- and *trans*-alkenes formed through AIBN mediated hydrosilylation of 1-hexyne with [tris(trimethyl)silyl]silane have almost identical ^{13}C chemical shifts, differing by only ~ 1 ppm.²⁸ The FTIR evidence (vide supra), however, suggests exclusive formation of the *cis*-olefin on porous silicon.

To verify that the two carbons appearing at 151 and 125 ppm in the porous silicon sample are indeed olefinic, the material was submitted to hydroboration. Addition of one of the B-H bonds across the olefin would result in its disappearance, thus demonstrating definitively through chemical means that the two peaks do correspond to a vinyl group. Room-temperature soaking of the pentenyl terminated porous silicon sample for 16 h in 1.0 M $\text{BH}_3 \cdot \text{THF}$ leads to the spectrum of Figure 3c in which the two peaks at 151 and 125 ppm are almost entirely absent, proving that this is clearly an olefin. The aliphatic region from 20 to 70 ppm becomes somewhat more complicated due to the conversion of the olefinic carbons to aliphatic methylene and organoborane species as a result of the reaction.²⁹ As observed by transmission FTIR, hydroboration also results in quantitative disappearance of the purported surface-bound vinyl group of the pentenyl moiety, as shown in Figure 1d.

To demonstrate that hydrosilylation also occurs with alkenes, a representative alkene, 1-pentene, was examined by NMR in a similar fashion. The soluble, molecular equivalent $[(\text{CH}_3)_3\text{Si}]_3\text{Si}(\text{CH}_2)_4\text{CH}_3$ was synthesized through an AIBN catalyzed addition of [tris(trimethyl)silyl]silane to 1-pentene. It was found that the EtAlCl_2 reaction proceeded only to $\sim 50\%$ conversion at best and was always heavily contaminated by the unreacted silane as a result. This result is not surprising since the hydrosilylation of alkenes with porous silicon is also sluggish, requiring longer reaction times than for alkynes and a large excess of olefin to drive the reaction. The solution phase ^{13}C NMR of $[(\text{CH}_3)_3\text{Si}]_3\text{Si}(\text{CH}_2)_4\text{CH}_3$ of Figure 3d is rather simple as expected: the five aliphatic carbons of the pentyl moiety appear at 36.5, 28.9, 22.2, 14.1, and 7.5 ppm and are accompanied by the nine methyls of the [tris(trimethyl)silyl]silane portion of the molecule at 1.2 ppm. The peak at 7.5 ppm corresponds to the carbon attached directly to the silicon since ^{29}Si coupling can be seen ($^1J_{\text{Si-C}} = 32$ Hz).

The most notable feature of the solid-state spectrum for the 1-pentene functionalized porous Si in Figure 3e is the chemical shift range of the observed resonances. There are apparently no olefinic resonances, and all of the observed lines are within the aliphatic/methyl region of the spectrum. The three sharp

(26) Sung, M. M.; Kluth, G. J.; Yauw, O. W.; Maboudian, R. *Langmuir* **1997**, *13*, 6164.

(27) (a) Yoshida, S.; Hanada, T.; Tanabe, S.; Soga, N. *J. Mater. Sci.* **1999**, *34*, 267. (b) Tsuboi, T.; Sakka, T.; Ogata, Y. H. *J. Electrochem. Soc.* **1999**, *146*, 372. (c) Tsuboi, T.; Sakka, T.; Ogata, Y. H. *Phys. Rev. B* **1998**, *58*, 13863. (d) Mamykin, A. I.; Moshnikov, V. A.; Il'in, A. Y. *Semiconductors* **1998**, *32*, 322. (e) Watanabe, A.; Fujitsuka, M.; Ito, O.; Miwa, T. *Jpn. J. Appl. Phys., Part 2* **1997**, *36*, L1265. (f) Petit, D.; Chazalviel, J.-N.; Ozanam, F.; Devreux, F. *Appl. Phys. Lett.* **1997**, *70*, 191. (g) Brandt, M. S.; Ready, S. E.; Boyce, J. B. *Appl. Phys. Lett.* **1997**, *70*, 188. (h) Chang, W. K.; Liao, M. Y.; Gleason, K. K. *J. Phys. Chem.* **1996**, *50*, 19653. (i) Pietrass, T.; Bifone, A.; Roth, R. D.; Koch, V. P.; Alivisatos, A. P.; Pines, A. *J. Non-Cryst. Solids* **1996**, *202*, 68. (j) Tennis, R. F.; Li, F.; Kirk, W. P. *Physica B* **1990**, *165* and *166*, 609.

(28) Kopping, B.; Chatgililoglu, C.; Zehnder, M.; Giese, B. *J. Org. Chem.* **1992**, *57*, 3994.

(29) It is expected that the borane will add to the least hindered carbon, that is, the carbon β to the surface silicon atom, but a mixture of α and β addition products cannot be ruled out. Pelter, A.; Smith, K.; Brown, H. C. *Borane Reagents*; Academic Press Limited: San Diego, 1988; pp 166-167.

Table 1. Relative Efficiencies [Decrease in ν (Si-H_x) Intensity] of the Hydrosilylation Reaction of Various Substrates as Determined by the % Decrease of Si-H_x Intensity by Transmission FTIR

	hydrosilylated substrate	average efficiency E (%) ^a
1	1-pentyne	19
2	1-dodecyne	17
3	2-hexyne	14
4	1-pentene	28
5	1-dodecene	28
6	<i>cis</i> -2-pentene	20
7	<i>trans</i> -2-hexene	11
8	2,3-dimethyl-2-pentene	11

^a Conditions: The efficiency is an average of 2–4 runs, with an error of $\pm 5\%$ of the calculated efficiencies. The porous silicon samples were prepared by etching procedure A (see Experimental Section).

resonances at 36.7, 22.9, 12.5 ppm (line widths ~ 200 Hz) compare well with the resonances observed in the liquid analogue spectrum. The peak near 28 ppm in the solid-state spectrum agrees with the liquid spectrum resonance appearing at 28.9 ppm. Line shape analysis also indicates that there is an additional, fifth resonance in the solid spectrum near 17.3 ppm [see Figure 3f].

The only major discrepancy between the solid-state and liquid-state NMR spectra comes from the assignment of the carbon directly bound to the surface silicon atom. For the liquid-state analogue, this resonance was found to be at 7.5 ppm and is noticeably absent in the solids spectrum. However, the solid-state spectrum contains a broad resonance (~ 700 Hz) that appears at 17.3 ppm. This resonance is likely to be the carbon bonded directly to porous Si, broadened by the heterogeneity of the surface sites. It is also plausible that the two broad resonances at 17.3 and 27.9 ppm (line width ~ 650 Hz) are composed of signals from several carbon environments, indicating the possibility of both Markovnikov and anti-Markovnikov hydrosilylation addition pathways. This latter possibility is also supported by the ²⁹Si spectrum (see Supporting Information), which contains two additional resonances at -12.5 and -49.8 ppm (relative to TMS) that are not present in the spectrum for untreated, porous Si. Double and triple resonance ¹³C-²⁹Si NMR experiments are planned that should shed considerably more light on the detailed nature of the bonding of such organic species to the porous Si surface.

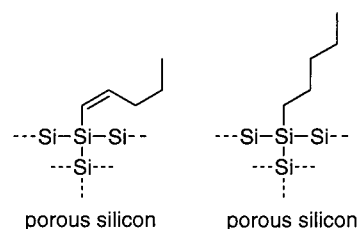
Surface Functionalization with Alkynes and Alkenes of Differing Substitution Patterns: Reaction Scope. The observed integrated intensity of the Si-H_x ($x = 1,2,3$) region diminishes following hydrosilylation, indicating consumption of Si-H bonds of the surface to afford the covalent attachment. Different substrates lead to consistent variation in the amount of decrease, suggesting that the efficiency of the reaction is related to the alkyne or alkene. The Si-H_x stretch region can therefore be used as a relative index of reaction progress in absorbance mode FTIR. The efficiency E is related to the change in the integrated intensity A of the Si-H region ($2000\text{--}2200\text{ cm}^{-1}$) after the hydrosilylation:

$$E = (A_0 - A_1)/A_0$$

where A_0 and A_1 are the baseline to peak areas of the freshly etched sample and the hydrosilylated sample, respectively. The data in Table 1 allow a comparison of the reaction efficiencies under the assumption that the intensities of the various hybridizations of the Si-H_x bonds are approximately the same, and that adjacent bonding of alkyl groups will not change the relative intensities. Although the $\sim 2110\text{ cm}^{-1}$ peak broadens to a certain degree after reaction, this can be expected due to

lowering of local order at the surface and an increase in chemical variability. In many cases, the exact mode(s) of Si-H addition is (are) ambiguous. For instance with 2-hexyne, the silicon atom may bind to either the 2- or 3-position, as has been seen for the solution phase hydrosilylation of this substrate with triethylsilane.¹⁸ Unfortunately, FTIR cannot distinguish easily between a mixture of two very closely related species and thus these ratios remain undetermined. By comparing the % consumption of Si-H_x groups, however, the overall relative efficiency of the hydrosilylation reaction can be determined, allowing for meaningful comparison between different substrates.

To summarize Table 1, the hydrosilylation reaction is sensitive to the regiochemistry and stereochemistry of the substrate molecule. The overall efficiency of alkenes is greater than alkynes, presumably because the *cis* stereochemistry of the resulting alkenyl group on the surface formed through alkyne hydrosilylation occupies more space than the corresponding alkyl group with the same number of carbons and cannot pack as well.



A comparison of entries 1 and 4 in Table 1 which contrast the efficiency E for 1-pentyne and 1-pentene reveal 19 and 28% efficiencies, respectively. The length of the alkyl chain has only minor effects on the efficiencies, as shown by entries 1 and 2 for 1-pentyne and 1-dodecyne. A clear distinction can also be made between *cis*- and *trans*-alkenes: examination of *cis*-2-pentene and *trans*-2-hexene as substrates indicates lower efficiency (entries 6 and 7: 20% vs 11%) and slight oxidation occurred with the *trans*-2-hexene sample, while reaction with the *cis*-2-pentene showed no oxidation. Internal alkynes incorporate less readily as compared with terminal alkynes, as shown through the hydrosilylation of 1-pentyne and 2-hexyne (entries 1 and 3: 19 vs 14%), and minor oxidation in the case of the internal alkyne. Hydrosilylation of the tetrasubstituted olefin 2,3-dimethyl-2-pentene is possible but gave similar minor oxidation and showed one of the lowest hydrosilylation efficiencies (11%). The minor oxidation noted could be due to a decreased reaction rate with the more sterically hindered substrates which allows oxidation caused by trace O₂ or H₂O to compete. Alternatively, the creation of strained surface bonded species due to the high steric requirements of the organic fragments may react rapidly upon exposure to air.

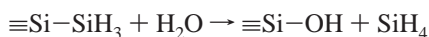
Although the limiting factor for the hydrosilylation is not known, the remaining IR-apparent Si-H bonds are inaccessible to catalytic hydrosilylation. After a sample was hydrosilylated with 1-dodecyne ($E_1 = 18\%$), quenched, rinsed, and scanned in the FTIR, it was immediately subjected to the hydrosilylation treatment again. After the second reaction procedure, no further Si-H consumption or incorporation of dodeceny groups was observed in the FTIR spectrum ($E_2 = 0\%$). It has been suggested previously that solution phase hydrosilylation with aluminum based Lewis acids proceeds through an intermediate involving a silane-Lewis acid complex which is then attacked by the alkyne/alkene.¹⁸ Treatment of the porous silicon surface with EtAlCl₂ and then washing gently with hexanes before adding

the alkene leads to no reaction, indicating that this purported interaction between the catalyst and surface Si–H residues is weak.

Stability of Hydrosilylated Surfaces: Chemical Resistance, Chemography, and FTIR Monitoring in Ambient Air. The native Si–H terminated porous silicon surfaces do not provide adequate stability for most potential applications of the material. Stabilization of porous silicon through introduction of a tunable monolayer would be extremely useful not only for technological applications, but for fundamental study of the origin of the observed light emission properties and quantum confinement effects of the embedded silicon nanocrystallites as well.

As demonstrated previously, hydrophobic porous silicon surfaces hydrosilylated with long chain or aromatic alkynes and alkenes are resistant to hydrolysis over a wide range of pH.¹⁴ We reported that a dodecanyl-terminated surface can withstand at least 4 h of boiling in an aerated aqueous KOH solution of pH 10. To further test the resistance of the derivatized material to basic treatment, the range of pH from 10 to 14 has been investigated. Because pH 13–14 is often utilized in existing silicon-based chip manufacturing processes, an understanding of the behavior of derivatized porous silicon at in this higher pH range is essential. As shown in Figure 4a, little appearance of oxidation is noted when either a 1-dodecyne or 1-dodecene treated porous silicon surface (etching procedure A) is boiled for 30 min at pH 12; as expected, identical spectra result from boiling 30 min in pH 10 and 11 KOH solutions. At pH 13, however, the porous silicon layer detaches from the bulk silicon, the particles of which are then observed to float on the solution surface. The porous layer is able to withstand 5 min of boiling at pH 13 with little oxidation as shown in Figure 4b. At pH 14, 5 min of boiling results in appearance of the ν (Si–O) stretch although the IR profile remains essentially unchanged [Figure 4c]. After 5 min, however, rapid fragmentation and detachment of the porous layer occurs. To contrast with the behavior of the native, Si–H terminated sample, destruction of the porous layer occurs in \sim 3, 2, 0.75, 0.33, and 0.25 min at pH 10, 11, 12, 13, and 14, respectively. The FTIR profile of an Si–H terminated sample of porous silicon after 5 min of boiling in pH 14 KOH is shown in Figure 4d. Complete disappearance of the ν (Si–H_x) centered around 2100 cm⁻¹ is observed, demonstrating that these unprotected surfaces are thoroughly destroyed under these conditions. Therefore, functionalization with long alkyl chains results in a dramatic lengthening of the possible exposure time of porous silicon to caustic basic treatment.

Oxidation of native Si–H terminated porous silicon in ambient air commences in tens of minutes and as a result, the surface characteristics, luminescence behavior, resistivity of the porous layer, and a host of other features continually change with time.³⁰ In 1994, Canham and co-workers demonstrated that porous silicon emits gaseous silanes in air which create images on photographic plates through reduction of the silver halide in the photographic emulsion.²² Silane emission is due to hydrolysis of the Si–SiH₃ bond, releasing SiH₄.



Because the increase in optical density of the spot will depend on the rate of silane emission from the porous silicon, chemography of porous silicon could qualitatively serve as a rapid screening technique of the relative rates of deterioration. As a comparison, Si–H and dodecanyl-terminated porous silicon

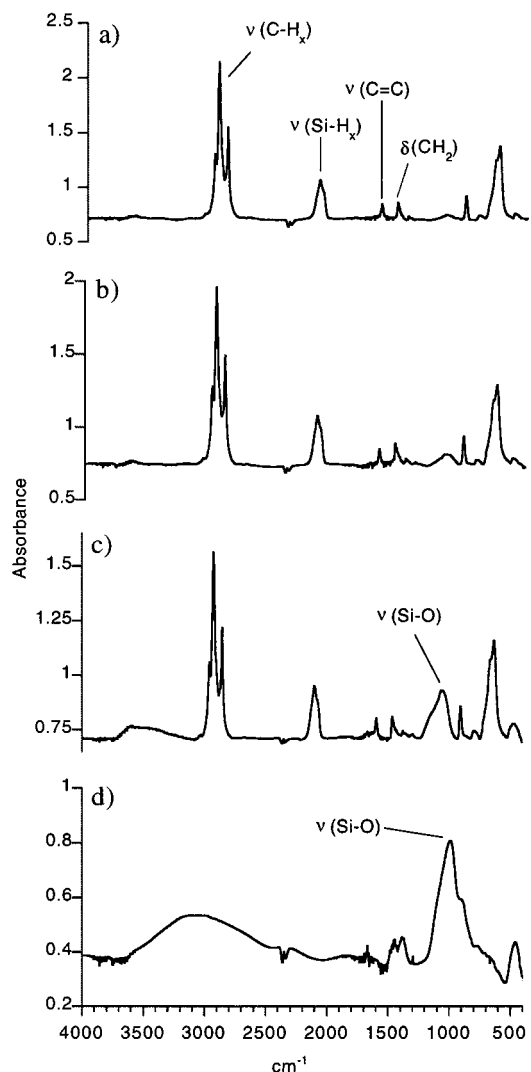


Figure 4. Stability studies of porous silicon (etching procedure A) upon boiling in aqueous, aerated solutions of pH 12–14: (a) 30 min boiling of a dodecanyl-terminated surface in pH 12 solution; (b) 5 min boiling of a dodecanyl-terminated surface in pH 13 solution; (c) 5 min boiling of a dodecanyl-terminated surface in pH 14 solution. (d) 5 min boiling of a native, hydride-terminated porous silicon sample in pH 14 solution.

samples derived from p⁻-type silicon (etching procedure B) were compared in an environment of 100% humidity, as shown in Figure 5. After 1 h, the Si–H terminated sample has heavily reduced the photographic plate, leading to a dark spot. The dodecanyl-derivatized sample, however, leaves only a very faint trace, indicating that the rate of silane emission from this sample is much slower. Only after a 4 h exposure time does the dodecanyl terminated surface begin to show a light, circular pattern. These results point to two possible effects of the surface hydrosilylation reaction: (i) the rate of hydrolysis of the surface Si–Si bonds is greatly diminished, leading to substantially less surface oxidation as indicated by the long-term FTIR studies, and/or (ii) that the hydrosilylation reaction consumes a large fraction of the surface hydrides on –SiH₃ substituents, leading to an overall reduction in the quantity of silanes that can be released. Even if a –SiH₃ substituent were converted to a –SiR₃ substituent, the resulting silane, R₃SiH, would still be expected to reduce the photographic plate if the Si–Si bond, through which it is bound to the surface, were to hydrolyze.

(30) (a) Grosman, A.; Ortega, C.; Siejka, J.; Chamarro, M. *J. Appl. Phys.* **1993**, *74*, 1992. (b) Grosman, A.; Ortega, C. In *Properties of Porous Silicon*; Canham, L. T., Ed.; INSPEC: London, 1997; p 145–153.

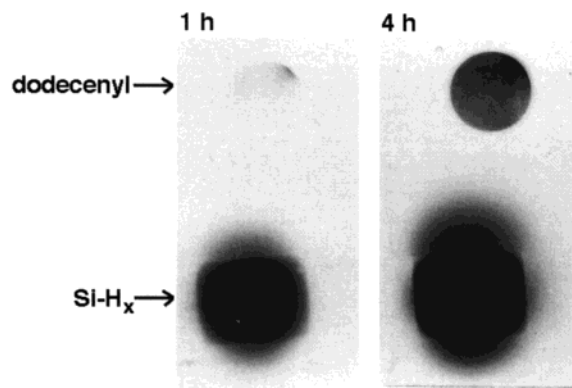
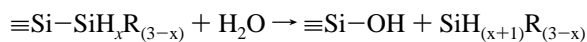


Figure 5. Chemography studies of dodecenyl- and silicon hydride-terminated porous silicon under 100% humidity after 1 and 4 h exposures. The top sample in each frame is the dodecenyl-terminated surface, while the bottom sample corresponds to the underivatized sample.



Thus, it appears that the chemography results point to a dramatically reduced rate of surface hydrolysis and oxidation under ambient conditions upon derivitization with a long chain hydrophobic monolayer.

To supplement the short-term chemography data with actual long-term studies done in ambient air in the absence of light, the formation of oxygen back-bonded Si-H_x moieties in freshly etched porous silicon samples derived from p-type wafers (etching procedure C) was examined. Porous silicon terminated with Si-H and dodecyl and dodecenyl groups was left under ambient conditions in air and FTIR spectra were taken periodically over 114 days. The samples were held during this time in an IR cell to directly compare intra-sample intensities accurately. The relative rate of formation of oxygen back-bonded ν (Si-H_x) centered around 2240 cm⁻¹ versus the disappearance of native, non-oxidized Si-H_x at 2100 cm⁻¹ was contrasted. With these hydrosilylated samples, ~17 and 28% of the silicon-hydrides are consumed for 1-dodecyne and 1-dodecene, respectively, and thus incorporation of surface oxide can be observed through formation of oxygen back-bonded Si-H groups of the remaining 83 and 72% of surface hydrides. As shown in Figure 6a, only the ν (Si-H_x) stretches can be seen in the freshly etched hydride-terminated sample. After 114 days, however, the intensity of the O₃SiH and O₂SiSiH stretches equals that of the non-oxygen back-bonded silicon-hydrides. In contrast, the porous silicon surfaces hydrosilylated with 1-dodecyne in Figure 6b shows only weak oxygen back-bonded ν (Si-H_x) stretches after 114 days, indicating little apparent incorporation of surface oxide. The 1-dodecene treated surface gave an almost identical profile as compared to 1-dodecyne, as shown in the Supporting Information.

Effect of the Hydrosilylation Reaction on Porous Silicon Morphology. An important factor that must be considered is whether the reaction induces any major changes in the morphology of the material. To demonstrate that the reaction takes place exclusively on the surface and does not promote rearrangement of the porous structure, measurements of surface area and average pore size before and after the reaction were taken. Large alterations in these data would indicate a restructuring or degradation of the silicon skeleton. Hydrosilylation of the small alkyne, 1-pentyne, was chosen as the test reaction since it should bring about only small decreases in surface area and pore size through formation of a thin monolayer on the surface. Free-

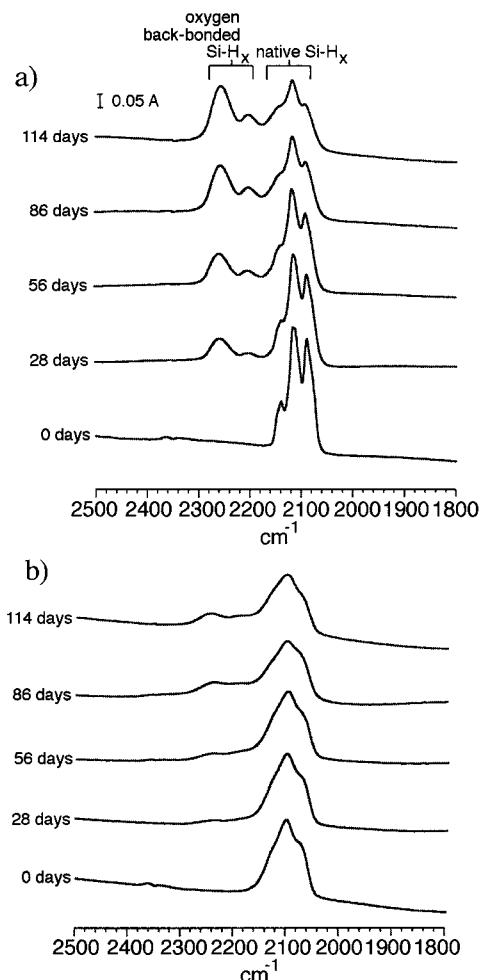


Figure 6. Long-term oxidation studies of the Si-H_x region of hydride- and dodecenyl-terminated surfaces in ambient air. (a) The native, hydride-capped surface. (b) The dodecenyl-terminated surface.

standing porous silicon layers, identical to those utilized for the solid-state NMR measurements, were prepared from p⁺ silicon according to etch D(b) in the Experimental Section. A free-standing Si-H terminated porous silicon disk of a diameter of 2.4 cm was split in half; one side was left as is and the other hydrosilylated with 1-pentyne. By using the same sample in this manner, inter-sample variation due to slight deviations from one preparation to another is avoided. Brunauer-Emmett-Teller (BET) and Barrett-Joyner-Halenda (BJH) nitrogen adsorption/desorption analyses were then carried out.¹⁶ No dramatic effects on either the surface area nor average pore size were noted. The surface area (BET) and average pore size (4V/A by BET) of the native silicon-hydride terminated surface before hydrosilylation were 262 m²/g and 14.1 nm, respectively. Upon hydrosilylation with 1-pentyne, slight decreases in surface area and pore size to 237 m²/g and 12.9 nm were noted, as would be expected by capping the pore walls with a short organic fragment.³¹ These results indicate that the porous structure is mainly unaffected by the hydrosilylation chemistry.

Because porous silicon is a heterogeneous, anisotropic material, the extent of hydrosilylation within the porous structure needs to be determined. If the hydrosilylation only occurs on the surface layer, then the utility of functionalized porous silicon for applications such as biosensors is extremely limited since the vast surface area of the material would be underutilized.

(31) The corresponding pore sizes by BJH before and after hydrosilylation are 13.7 and 12.7 nm, respectively.

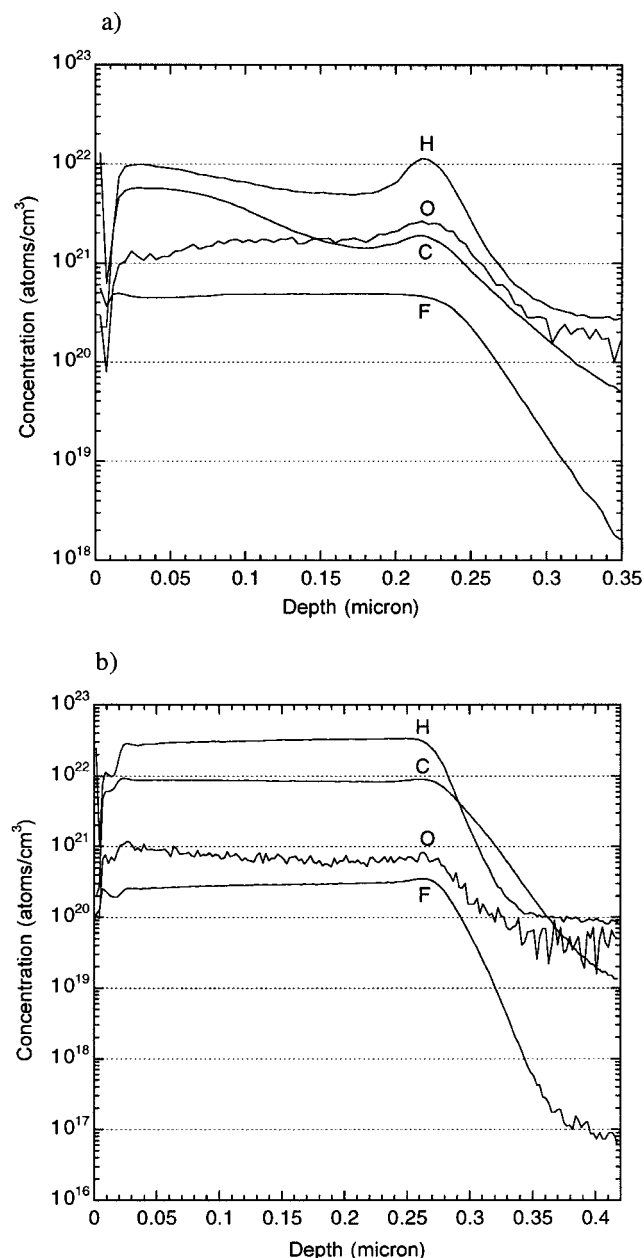


Figure 7. Depth-profiled secondary ionization mass spectra (SIMS) of (a) the native, hydride-capped surface and (b) a dodeceny-terminated surface of an otherwise identical mesoporous layer, fabricated by etching procedure B.

To determine the distribution of the organic moieties derived from the hydrosilylation reaction through the porous material, secondary ionization mass spectrometry (SIMS) depth profiling experiments were carried out on Si-H, dodecyl-, and dodeceny-terminated porous silicon. A 275 nm thick porous silicon sample formed through etching procedure B was cut in half; one-half was left underivatized and the remaining half hydrosilylated with 1-dodecene. As can be seen by comparing Figure 7a and b, the amount of carbon observed increases substantially upon hydrosilylation. Importantly, Figure 7b indicates that the level of carbon throughout the sample is remarkably constant, showing that the hydrosilylation reaction does not take place exclusively on the surface layer. Rather, excellent penetration by the hydrophobic reagents, EtAlCl_2 and 1-dodecene, allows for consistent functionalization down the length of the pore. An almost identical set of profiles is observed with a 1-dodecyne reacted surface (Supporting Information). Because the surface

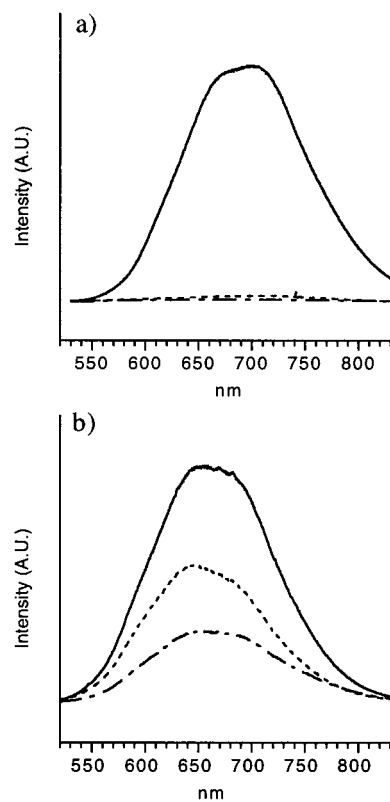


Figure 8. Photoluminescence spectra. Photoluminescence spectrum: (—) before functionalization (hydride-terminated); (---) following hydrosilylation, and (···) hydrosilylated surface after a 30 min soak in a 1:1 49% HF (aqueous)/EtOH solution. (a) Hydrosilylation of phenylacetylene, yielding a styrenyl-terminated surface. (b) Hydrosilylation of 1-dodecene, yielding a dodecyl-terminated porous silicon.

area of these porous silicon samples was not determined due to the thinness of the sample, these SIMS spectra cannot be used to determine an exact elemental analysis.

Influence of Surface Termination on Photoluminescence.

The influence of the hydrosilylation reaction on the light-emitting properties has been investigated. Previously, the termination of porous silicon has been demonstrated to play a very important role in the photoluminescence efficiency of porous silicon.^{12a,b,32,33} The effects of hydrosilylation of 1-dodecyne, 1-dodecene, and phenylacetylene on the photoluminescence of n-type porous silicon prepared through etch A were examined since these three substrates result in different classes of terminations — alkyl, vinyl, and conjugated vinyl. As we and others have previously noted, conjugation of a phenyl through either a vinyl³³ or alkynyl^{12a} unit is highly detrimental to the photoluminescence efficiency, as shown for the styrenyl termination in Figure 8a, produced through hydrosilylation of phenylacetylene. An extended 30 min soaking in HF does not bring about any photoluminescence recovery. The dodecyl (shown in Figure 8b) and dodeceny derivatized surfaces, produced through hydrosilylation of 1-dodecene and 1-dodecyne, respectively, both show a reduction in photoluminescence efficiency to about 25 and 15%, respectively, as compared to the freshly etched samples terminated with SiH_x . On the other hand, 30 min of contact with HF in room light induces partial restoration of the photoluminescence in both cases, as demonstrated in Figure 8b and the Supporting Information. In the case of the 1-dodecene- and 1-dodecyne-treated surfaces, the pho-

(32) Lauerhaas, J. M.; Sailor, M. J. *Science* **1993**, *261*, 1567.

(33) Buriak, J. M.; Allen, M. J. *J. Lumin.* **1999**, *80*, 29.

photoluminescence returns to 58 and 37% of the observed intensity before functionalization, respectively. This effect has been previously observed for freshly etched SiH_x-terminated porous silicon and may be due to a light-induced, secondary, in situ etch,^{34,35} a conclusion substantiated by the fact that the 1-dodecyl-treated surface only shows a restoration of photoluminescence intensity to 21% in the dark, as opposed to 37% in the light. Comparison of FTIR spectra before and after HF treatment reveals no significant changes in intensity of the ν (Si-H_x) stretch, however, suggesting that the amount of etching achieved under these conditions is low as compared to the already high surface area of the electrochemically etched surface. When a 1-dodecyl-treated surface is exposed to an analogous ethanolic solution of HCl in either room light and in the dark for 30 min, the photoluminescence increases only 6% above that observed for the functionalized surface. This result indicates that acid-base neutralization of surface defects, potentially responsible for photoluminescence quenching, may play a minor role under these conditions.³⁶

Conclusions

Hydrosilylation of alkynes and alkenes is efficiently mediated by the Lewis acid EtAlCl₂ on hydride-terminated porous silicon surfaces, yielding alkenyl and alkyl derivatization, respectively. The olefin of the alkenyl terminated surface appears to have (*Z*) *cis* geometry since it results from *trans* addition of the Si-H group, as is the case with the equivalent solution-phase reaction. Detailed FTIR analyses were corroborated by ¹³C solid-state NMR experiments which substantiate the claim for silicon-carbon formation on the surface. Long-term stability studies under ambient laboratory conditions reveal that the surfaces hydrosilylated with 1-dodecyl and 1-dodecene are stabilized with respect to hydrolysis and oxidation, compared to native hydride-terminated samples. The release of silanes from the surface as a result of hydrolysis is dramatically decreased due to the increased resistance of the hydrophobic, hydrosilylated samples. The hydrosilylation reaction appears to affect the surface of porous silicon and not the nanocrystalline skeleton since the surface area and average pore size decrease only slightly due to the coating of the pore interiors with the organic monolayer. Large changes in morphology are avoided, which is crucial for future technological applications of this functionalized material which utilize the intrinsic properties of the material, such as high surface area, quantum confinement effects of the nanocrystallites, and others. The hydrosilylation reaction takes place throughout the porous structure as determined by SIMS analyses as a result of the hydrophobic nature of the Lewis acid and alkynes. While hydrosilylation with 1-dodecyl and 1-dodecene result in quenching of about 75% of the photoluminescence intensity, soaking in HF solutions can bring about partial recovery. The hydrosilylation chemistry described above presents significant possibilities to address porous silicon in a wide range of devices and will continue to provide avenues to explore fundamental issues involving hydride terminated silicon surfaces.

(34) Li, K.-H.; Tsai, C.; Shih, S.; Hsu, T.; Kwong, D. L.; Campbell, J. C. *J. Appl. Phys.* **1992**, *72*, 3816.

(35) Noguchi, N.; Suemune, I. *Appl. Phys. Lett.* **1993**, *62*, 1429.

(36) Yablonovitch, E.; Allara, D. L.; Chang, C. C.; Gmitter, T.; Bright, T. B. *Phys. Rev. Lett.* **1986**, *57*, 249.

Experimental Section

General Methods. THF and CH₂Cl₂ were purified using the Grubbs/Dow Chemical solvent purification system.³⁷ Water (18 M Ω) was purified with a Millipore filtration system. All alkynes and alkenes were sparged with dry nitrogen or argon, filtered over anhydrous alumina under inert atmosphere to eliminate water and peroxides, and stored at -35 °C under nitrogen in absence of light. Air-sensitive procedures were carried out in a nitrogen-filled Vacuum Atmospheres glovebox (<1 ppm H₂O, O₂) or with standard Schlenk techniques (ChemGlass grease-free dual manifold vacuum/argon lines). Hydrosilylation of 1-pentyne and 1-pentene with molecular silanes, mediated by EtAlCl₂ or AIBN, was carried out according to previously published procedures.^{18,26,28c} The pH was measured with a Cole Parmer instrument, model number 59002-00.

FTIR Spectra. A Perkin-Elmer 2000 FTIR spectrometer was used to collect the porous silicon spectra in transmission mode against a crystalline silicon background with a nitrogen purge. Sixteen scans were accumulated with a typical spectral resolution of 4 cm⁻¹.

NMR Spectra. Solution-phase NMR spectra were obtained on either a Varian Gemini 200 MHz or INOVA 300 MHz instrument. The solid-state NMR experiments were carried out on a Varian Unity Plus 300 MHz spectrometer using a Chemagnetics MAS probe. Approximately 120 mg of sample was loaded into a 5 mm pencil rotor and was spun at frequencies of 5-7 kHz. Solid-state ¹³C spectra were obtained using ¹H-¹³C cross polarization with ¹H t_{90} 2.75 μ s and contact pulse widths of 1-2.5 ms. The ¹H T_1 's were relatively short, (1-3 s), allowing recycle delays of 3-5 s. Approximately 7000-10000 scans were accumulated for each solid-state spectrum. Linear prediction was used on the first three complex data points of each spectrum to remove a broad probe background peak centered at 110 ppm. The ¹³C resonances are reported relative to TMS by use of an external reference to HMB (hexamethylbenzene), taking the aromatic peak to be 132.2 ppm downfield from TMS.

Photoluminescence. Photoluminescence (steady state) measurements were carried out with an Oriel 250 W mercury arc lamp and a Bausch and Lomb monochromator set to 440 nm with a 450 nm SWP filter (CVI SPF450) as the excitation source, giving an intensity of 0.2 mW/cm² at the sample. Luminescence was passed through a 490 nm LWP filter (CVI LP490) into an Acton Research Spectra Pro 275 0.275 m monochromator and a Princeton Instruments LN₂ cooled CCD detector, model LN/CCD-1024-E/1.

Surface Area/Pore Size Measurements. BJH and BET measurements were carried out on a Micromeritics Accelerated Surface Area and Porosimetry System (ASAP) 2000. The porous silicon samples were pretreated at 150 °C under vacuum for 24 h before analysis.

Secondary Ionization Mass Spectrometry. SIMS measurements were carried out on a Cameca IMS 4F instrument using a 10 nA 10 kV Cs⁺ ion beam, a rastered crater size of 150 μ m diameter, with a central analysis area of 12 μ m diameter.

Chemography. Porous silicon samples with an area of 1.1 cm² were prepared through etching procedure B and were functionalized according to the standard hydrosilylation procedure outlined below. The chemographs were taken using 25 μ m thick Ilford L4 nuclear tracking emulsion plates. Porous silicon samples were placed in direct contact with the plate in air of 100% relative humidity at room temperature for times ranging from 1 to 4 h in complete darkness. The plates were then presoaked in deionized water, developed using 3:1 diluted Kodak D19 developer for 5 min and 30 s, and fixed in 7:1 diluted G333C AGFA for 30 min. All of these operations were conducted at 5 °C. Subsequent washing in water for 1 h was carried out at room temperature. The plates were then printed onto photographic paper using a Fuji Pictostat 300 running in transmission mode so that the black features shown here correspond to high exposure in the original plate.

Porous Silicon Etching Procedures. Because different analytical techniques were better suited toward different porous silicon morphologies and quantities, five different etching procedures were followed. The known physical characteristics of the porous silicon material is

(37) Pangborn, A. B.; Giardello, M. A.; Grubbs, R. H.; Rosen, R. K.; Timmers, F. J. *Organometallics* **1996**, *15*, 1518.

also described. In all cases, prime grade wafers of the (100) orientation are utilized (Transition Technology International).

Etching Procedure A. Photoluminescent silicon samples were prepared under ambient air according to previously published procedures through a galvanostatic etch.³⁸ A 0.28 cm² or 1.1 cm² exposed area of a polished, crystalline n-type silicon wafer (prime grade, P-doped, 0.70 Ω·cm) was etched for 3 min in a Teflon cell at 75 mA/cm² (positive bias) under 30 mW/cm² white light illumination, derived from a 300 W tungsten filament ELH bulb using 1:1 49% HF (aqueous)/EtOH as the electrolyte/etchant. After etching, the porous silicon samples were rinsed copiously with ethanol followed by pentane, and dried under a gentle nitrogen flow.

Etching Procedure B. This etch yields thin (~275 nm thick), smooth and homogeneous samples which were utilized for chemography and SIMS applications. P⁻ silicon (7.5–8.5 Ω·cm, B doped) is etched in a 1.1 cm diameter Teflon cell using the following conditions: 2 mA/cm² for 5 min in the dark with a 1:1 49% HF (aqueous)/EtOH etching solution. The samples were rinsed with EtOH and, without allowing drying of the surface, were rinsed copiously with pentane to prevent capillary action from damaging the silicon architecture.³⁹

Etching Procedure C. For the long-term stability studies, porous silicon derived from p⁻ type silicon was utilized. The porous layer of these samples is thick enough to yield a significant absorbance for the chemisorbed organic groups, and give well defined, sharp Si–H_x stretches with little IR absorbance due to doping. P⁻ silicon (7.5–8.5 Ω·cm, B doped) wafers are etched in 0.28 cm² or 1.1 cm² Teflon etching cells in the dark for 30 min at a current density of 7.1 mA/cm² with a 1:1 49% HF (aqueous)/EtOH etching solution. As in etching procedure B, the surfaces are rinsed with pentane to prevent cracking of the porous silicon skeleton.

Etching Procedure D. This etch provides large quantities of free-standing porous silicon samples for characterization via analytical techniques which require substantial masses. P⁺ silicon (0.010 Ω·cm, B doped) is etched in either a (a) 1.2 cm or (b) 2.4 cm diameter Teflon cell using the following conditions. For (a): 37 mA/cm² for 3 h with a 1:1 49% HF (aqueous)/EtOH etching solution, recycling the etching solution every 20 min without shorting the current cell, followed by a short, high-current etch of 0.4 A/cm² for 5 min to release the porous layer, resulting in a free-standing disk with a thickness of 300 μm (as measured with a micrometer) and a mass of approximately 30 mg. The samples were rinsed with EtOH and then pentane. Gravimetry indicated a porosity of 60–70%.⁴⁰ For (b): current density, HF cycling and rinsing procedures are kept the same but the etching duration is reduced to 1 h. This yields 30 mg of material with a thickness of 10 μm and a porosity, as determined by gravimetry, of 55%. As determined by BET measurements, the surface area and average pore diameter are ~260 m²/g and 14 nm, respectively. Preparation (a) is used for solid-state NMR, and preparation (b) for BET/BJH measurements.

Etching Procedure E. According to literature precedent, this preparation yields microporous porous silicon.⁴¹ P⁻ silicon (7.5–8.5 Ω·cm, B doped) wafers are etched in 0.28 cm² or 1.1 cm² Teflon etching cells in the dark for 30 min at a current density of 7.1 mA/cm² with a 49% HF (aqueous) etching solution. As in etching procedure B, the surfaces are rinsed with pentane to prevent cracking of the porous silicon skeleton.

EtAlCl₂ Hydrosilylation on Porous Silicon. Hydrosilylation reactions were carried out according to the following general procedure: a porous silicon sample is brought into the glovebox in a round-bottom flask, and then the flask is sealed with a septum. A 1.0 M hexane solution of EtAlCl₂ (Aldrich) was dropped onto the wafer surface with a microliter syringe through the rubber septum, followed by addition of the alkene or alkyne, also via the rubber septum with a microliter syringe. The reaction was left to react at room temperature: alkynes for 1 h, and alkenes for at least 12 h. Afterward, the sample was

quenched under inert atmosphere with THF, followed by CH₂Cl₂, and then removed to laboratory atmosphere, rinsed in air with EtOH, and dried under an N₂ stream. The actual amounts of the EtAlCl₂ solution and alkyne/alkene depend on the wafer size and volatility of the substrate, as described here. For porous silicon areas of 0.28 cm² or 1.1 cm² utilizing relatively involatile alkynes or alkenes (bp > 60 °C): 10 μL (10⁻⁵ mol) of the 1.0 M hexane solution of EtAlCl₂ and 3 μL of an alkyne or 50 μL of an alkene. For porous silicon areas of 0.28 cm² or 1.1 cm² utilizing relatively volatile alkynes or alkenes (bp < 60 °C): 10 μL (10⁻⁵ mol) of the 1.0 M hexane solution of EtAlCl₂ and 100 μL of the alkyne or alkene. For porous silicon areas of 4.52 cm² (formed from the etching cell with a 2.4 cm diameter), free-standing or not and regardless of substrate volatility, 0.5 mL (5 × 10⁻⁴ mol) of the 1.0 M hexane solution of EtAlCl₂ and 0.4 mL of the alkyne or alkene. Alkynes were generally left to react 2 h, and alkenes at least 12 h.

Hydroboration. In all cases, the porous silicon sample was soaked in 2.0 mL of a commercially available 1.0 M BH₃·THF solution in THF (Aldrich) under inert atmosphere for 16 h. In the case of the free-standing porous layer, due to fragmentation of the fragile disk, the material was removed from the borane solution through 5 min of centrifugation (5000 rpm) and then washed with excess THF in a similar manner.

FTIR Spectral Data of Surfaces Prepared through EtAlCl₂-Mediated Hydrosilylation. The data below correspond to porous silicon samples prepared through etching procedure A. Regardless of the etching procedure used, however, the FTIR profiles are extremely similar.

1-Pentyne hydrosilylation: 2961 cm⁻¹ ν(CH₃), 2931 and 2876 cm⁻¹ ν(CH₂), 2100 cm⁻¹ ν(Si–H_x), 1595 cm⁻¹ ν(SiC=C), 1461 cm⁻¹ δ-(CH₂), 1379 cm⁻¹ δ(CH₃), 1070 cm⁻¹ ν(Si–O), 905 cm⁻¹ δ(SiH₂), 661 cm⁻¹ δ(SiH), 628 cm⁻¹ δ(SiH₂).

1-Dodecyne hydrosilylation: 2951 cm⁻¹ ν(CH₃), 2924 and 2855 cm⁻¹ ν(CH₂), 2103 cm⁻¹ ν(Si–H_x), 1596 cm⁻¹ ν(SiC=C), 1465 cm⁻¹ δ(CH₂), 1376 cm⁻¹ δ(CH₃), 1062 cm⁻¹ ν(Si–O), 903 cm⁻¹ δ(SiH₂), 661 cm⁻¹ δ(SiH), 623 cm⁻¹ δ(SiH₂).

2-Hexyne hydrosilylation: 2951 cm⁻¹ ν(CH₃), 2924 and 2855 cm⁻¹ ν(CH₂), 2103 cm⁻¹ ν(Si–H_x), 1596 cm⁻¹ ν(SiC=C), 1465 cm⁻¹ δ-(CH₂), 1376 cm⁻¹ δ(CH₃), 1062 cm⁻¹ ν(Si–O), 903 cm⁻¹ δ(SiH₂), 661 cm⁻¹ δ(SiH), 623 cm⁻¹ δ(SiH₂).

1-Pentene hydrosilylation: 2962 and 2871 cm⁻¹ ν(CH₃), 2925 and 2855 cm⁻¹ ν(CH₂), 2103 cm⁻¹ ν(Si–H_x), 1465 cm⁻¹ δ(CH₂), 1376 cm⁻¹ δ(CH₃), 1062 cm⁻¹ ν(Si–O), 903 cm⁻¹ δ(SiH₂), 661 cm⁻¹ δ-(SiH), 623 cm⁻¹ δ(SiH₂).

1-Dodecene hydrosilylation: 2944 cm⁻¹ ν(CH₃), 2923 and 2854 cm⁻¹ ν(CH₂), 2102 cm⁻¹ ν(Si–H_x), 1466 cm⁻¹ δ(CH₂), 1378 cm⁻¹ δ(CH₃), 903 cm⁻¹ δ(SiH₂), 666 cm⁻¹ δ(SiH), 626 cm⁻¹ δ(SiH₂).

cis-2-Pentene hydrosilylation: 2960 and 2872 cm⁻¹ ν(CH₃), 2925 and 2855 cm⁻¹ ν(CH₂), 2103 cm⁻¹ ν(Si–H_x), 1460 cm⁻¹ δ(CH₂), 1374 cm⁻¹ δ(CH₃), 1060 cm⁻¹ ν(Si–O), 904 cm⁻¹ δ(SiH₂), 662 cm⁻¹ δ-(SiH), 622 cm⁻¹ δ(SiH₂).

trans-2-Hexene hydrosilylation: 2959 and 2874 cm⁻¹ ν(CH₃), 2930 and 2850 cm⁻¹ ν(CH₂), 2103 cm⁻¹ ν(Si–H_x), 1461 cm⁻¹ δ(CH₂), 1380 cm⁻¹ δ(CH₃), 1055 cm⁻¹ ν(Si–O), 906 cm⁻¹ δ(SiH₂), 660 cm⁻¹ δ-(SiH), 625 cm⁻¹ δ(SiH₂).

2,3-Dimethyl-2-pentene hydrosilylation: 2966 and 2880 cm⁻¹ ν(CH₃), 2923 and 2854 cm⁻¹ ν(CH₂), 2110 cm⁻¹ ν(Si–H_x), 1454 cm⁻¹ δ(CH₂), 1380 cm⁻¹ δ(CH₃), 1059 cm⁻¹ ν(Si–O), 907 cm⁻¹ δ(SiH₂), 664 cm⁻¹ δ(SiH), 623 cm⁻¹ δ(SiH₂).

Styrene hydrosilylation: 3034 cm⁻¹ ν(CH) aromatic, 2930–2846 cm⁻¹ ν(CH₂), 2112 cm⁻¹ ν(Si–H_x), 1604 and 1492 cm⁻¹ ν(C=C) skeletal in-plane vibrations, 1450 cm⁻¹ δ(CH₂), 1064 cm⁻¹ ν(Si–O), 906 cm⁻¹ δ(SiH₂), 664 cm⁻¹ δ(SiH), 622 cm⁻¹ δ(SiH₂).

Phenylacetylene hydrosilylation: 3061–3026 cm⁻¹ ν(CH) aromatic, 2104 cm⁻¹ ν(Si–H_x), 1598, 1587, and 1567 cm⁻¹ ν(C=C) skeletal in-plane vibration + alkene ν(SiC=C), 1493 and 1444 cm⁻¹ ν(C=C) skeletal in-plane vibration, 1071 cm⁻¹ ν(Si–O), 902 cm⁻¹ δ(SiH₂), 662 cm⁻¹ δ(SiH), 629 cm⁻¹ δ(SiH₂).

Thermal Hydrosilylation of 1-Dodecyne. A sample of porous silicon prepared through etching procedure A was covered with 5.0 mL of neat 1-dodecyne under argon and refluxed for 2 h. After cooling

(38) Lee, E. J.; Bitner, T. W.; Ha, J. S.; Shane, M. J.; Sailor, M. J. *J. Am. Chem. Soc.* **1996**, *118*, 1390.

(39) Bellet, D. In *Properties of Porous Silicon*; Canham, L. T., Ed.; INSPEC: London, 1997; p 38–43.

(40) Halimaoui, A. In *Properties of Porous Silicon*; Canham, L. T., Ed.; INSPEC: London, 1997; pp 12–22.

(41) Canham, L. T.; Groszek, A. *J. Appl. Phys.* **1992**, *72*, 1558.

to room temperature, the dodecyl-terminated sample was washed extensively with CH_2Cl_2 and dried under an N_2 stream.

Acknowledgment. J.M.B. thanks the NSF for a Career Award (1999–2003), the Camille and Henry Dreyfus Foundation for a New Faculty Award (1997–2002), the Petroleum Research Fund (administered by the ACS), and Purdue University for support. M.P.S. holds a Link Foundation pre-doctoral fellowship, and M.J.A. an undergraduate scholarship from the Purdue Alumni/Eli Lilly Foundation. Dr. Edward Robins is thanked for assistance with the solution phase ^{13}C NMR spectra and Dr. Jon P. Newey for carrying out the SIMS analyses. J. S. thanks the Lubrizol Corporation for a pre-doctoral fellowship. D.R. thanks the NSF for a Career Award (1998–2002), the

Research Corporation Cottrell Scholars program, and the A. P. Sloan Foundation (1999–2001) for support. L.T.C. was supported by the U.K. M.O.D. Corporate Research Program.

Supporting Information Available: IR spectra of 1-[tris-(trimethylsilyl)silyl]-(*Z*)-pentene and of a thermally hydrosilylated surface terminated with 1-dodecyl moieties demonstrating the $\gamma_{\text{w}}(-\text{CH}=\text{CH}-)_{\text{trans}}$, SIMS and PL spectra of a 1-dodecyl-terminated surface, additional details concerning BET/BJH data, and ^{29}Si CP/MAS spectra of $\text{Si}-\text{H}_x$ and pentyl terminated surfaces (PDF). This material is available free of charge via the Internet at <http://pubs.acs.org>.

JA992188W